

Supplementary Material

**Piezoresistive behavior of DLP 3D-printed CNT/polymer nanocomposites under
monotonic and cyclic loading**

Omar Waqas Saadi^a, Andreas Schiffer^{a,*}, S Kumar^{b,*}

^aDepartment of Mechanical Engineering, Khalifa University of Science and Technology,

Main Campus, P.O. Box 127788, Abu Dhabi, United Arab Emirates

^bJames Watt School of Engineering, University of Glasgow, Glasgow, G12 8LT, UK

* Corresponding authors: andreas.schiffer@ku.ac.ae (A. Schiffer), s.kumar@eng.oxon.org (S. Kumar)

S1. Microstructure analysis

X-ray Micro-Computed Tomography (μ CT) analysis was carried out to identify the presence of voids in the 3D printed nanocomposite using a Phoenix nanotom® M nanoCT 3D scanner (GE Sensing & Inspection Technologies GmbH). A prismatic PC-0.01 specimen with dimensions $12.5 \times 12.5 \times 25 \text{ mm}^3$ was scanned at a resolution of $10 \mu\text{m}$.

Selected μ CT scans of the nanocomposite with 0.01 phr MWCNT loading are presented in Fig. S1, showing the cross-section of the specimen at different locations. In the entire specimen, we could identify only one pore of size $\approx 10 \mu\text{m}$, suggesting that the 3D printed specimen had negligible porosity.

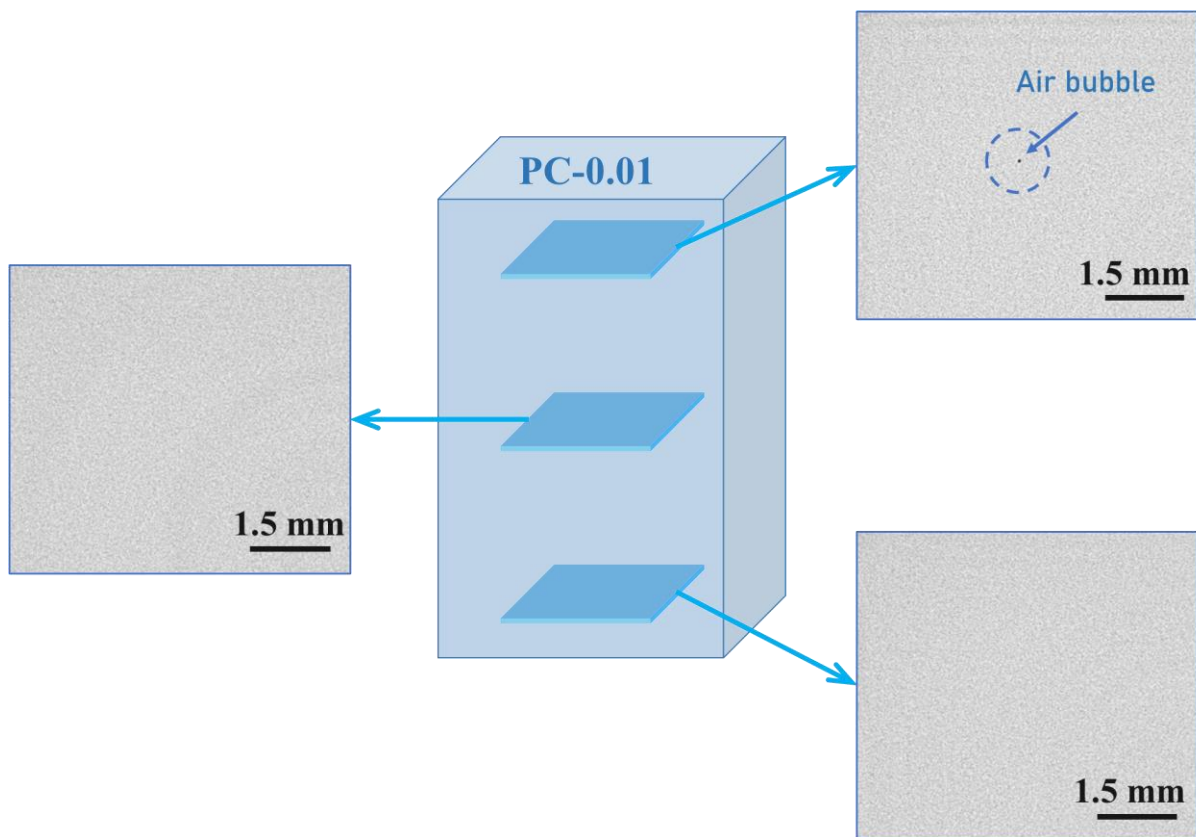


Figure S1. μ CT images of the 3D printed nanocomposite with 0.01 phr MWCNT loading.

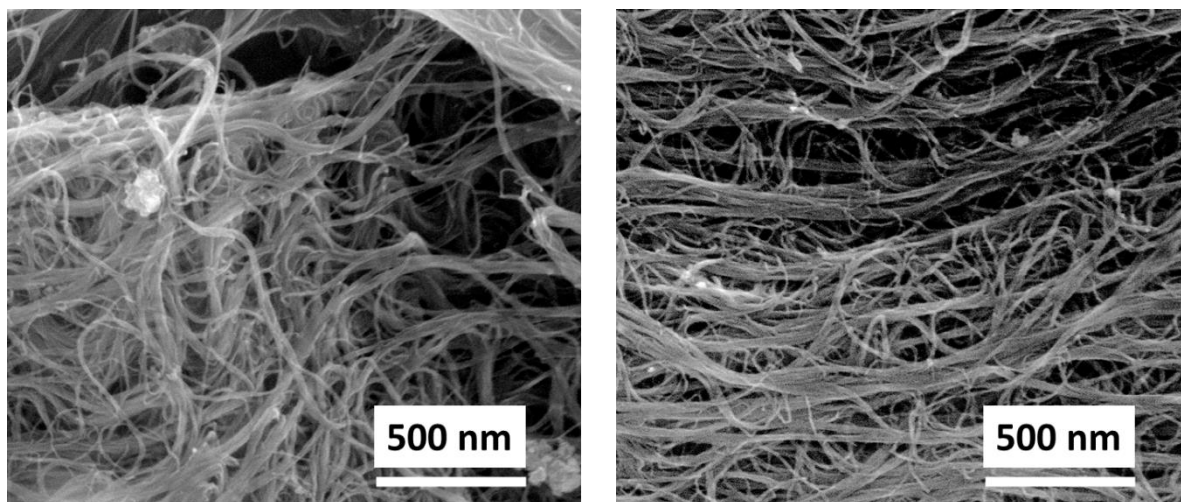


Figure S2. SEM images of the as-received MWCNTs.

High-resolution scanning electron microscopy (SEM) was used to analyze the morphology of the as-received MWCNTs. The SEM scans were performed using a scanning electron microscope (Nova NanoSEM 650, FEI Co., USA) with 7.5 kV accelerating voltage and are shown in Fig. S2. It is clear from the images that the MWCNTs are packed into bundles of variable thickness, forming a complex interconnected network.

S2. Dynamic mechanical analysis (DMA)

Dynamic mechanical analysis was performed using a DMA tester (Model 242 Artemis, NETZSCH, Selb, Germany) in bending mode to measure the storage and loss modulus of the MWCNT/polymer nanocomposites as a function of temperature. The temperature sweep was performed at 2°C/min in the range of 25-180°C.

In Fig. S3, we plot the storage modulus (E') and loss factor ($\tan \delta$) of the 3D printed neat polymer and MWCNT/polymer nanocomposites over a temperature range of $25^\circ\text{C} \leq T \leq 180^\circ\text{C}$. For all samples, the storage modulus initially decreased sharply and reached a plateau at 70-80°C which is a characteristic trend for thermoset polymers [1]. A reduction in the maximum storage modulus was observed with increasing MWCNT loading, possibly due to lower cross-linking density and insufficient curing by UV light, as mentioned in DSC analysis (see section 3.3.1 in the manuscript), and weak interfacial interactions between the MWCNTs and the nanofillers (see section 3.2 in the manuscript). The loss factor ($\tan \delta$) curves in Fig. S3 describe the damping behavior of the materials as a function of temperature. For all samples, the loss factors started at values > 0.1 , indicating that all materials exhibit viscoelastic behavior at room temperature. Furthermore, the $\tan \delta$ values at room temperature increase slightly with increasing MWCNT concentration, which is attributed to incomplete UV curing of the nanocomposites during 3D printing (see section 3.3.1 in the manuscript).

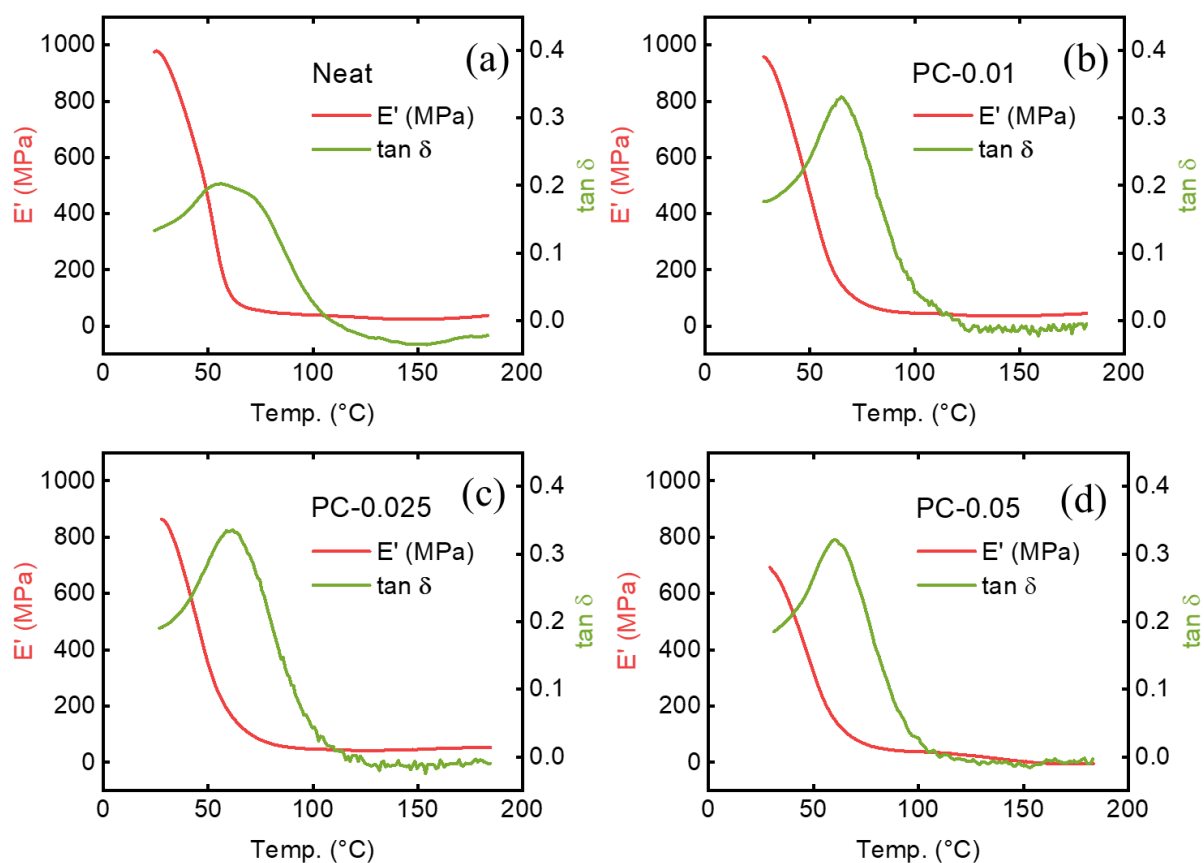


Figure S3. DMA curves of (a) neat specimen, (b) PC-0.01, (c) PC-0.025, and (d) PC-0.05 nanocomposites showing the storage modulus and loss factor as a function of temperature.

S3. Effect of printing parameters on the mechanical response

S3.1. Effect of layer thickness

To examine the effect of the DLP layer thickness on the mechanical properties of the neat PlasClear-TPGDA, tensile tests were performed on dogbone specimens (gauge section measuring 33 x 5 x 2 mm) printed in flat orientation with different layer thicknesses (0.025mm, 0.05 mm, 0.075 mm, 0.1 mm). For these tests, a Zwick-Roell universal testing machine (UTM) with a 2.5 kN load cell was used, and the cross-head speed was set to 2.5 mm/min. Each test was repeated seven times on virgin specimens to ensure that the results are repeatable. Note that the specimens with smaller layer thickness took a longer time to print because of the larger number of layers required to build the 2 mm-thick specimen.

The measured stress vs. strain curves of specimens with different layer thickness are plotted in Fig. S4a; the Young's modulus and ultimate strength values evaluated from these curves are presented in Fig. S4b. The results show that, by decreasing the layer thickness from 0.1 mm to 0.025 mm, the modulus and tensile strength increased by 38% and 24%, respectively. The reason for this increase is attributed to the fact that the resin in the specimens with smaller layer thickness was exposed to more UV light during 3D printing, and this increased the degree of cross-linking in the specimens. It should also be mentioned that the increase in modulus and strength resulted in a concomitant decrease in ductility, as evinced by the observed reduction in fracture strain.

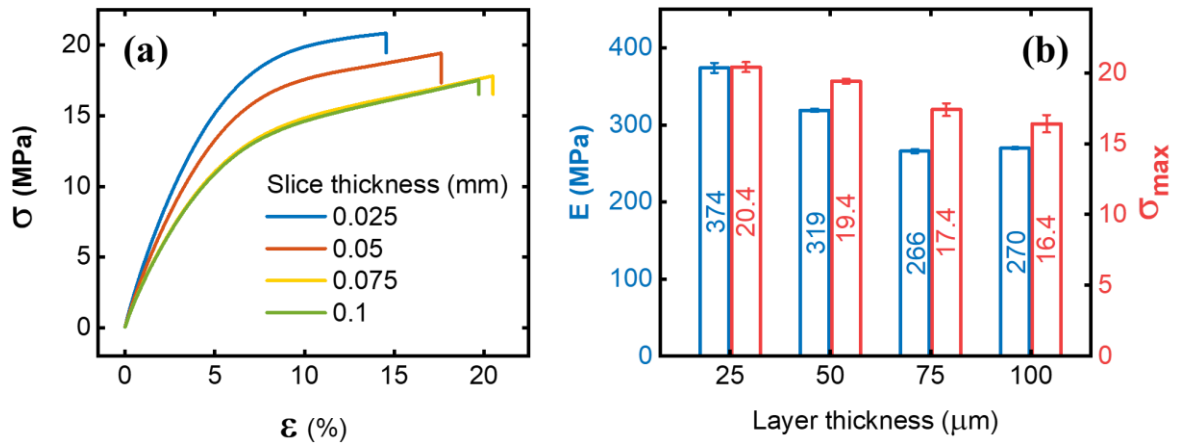


Figure S4. Effect of layer (or slice) thickness on the stress-strain behavior (a) and the measured mechanical properties (b) of neat PlasClear-TPGDA.

S3.2. Effect of build orientation

To study the effect of build orientation on the mechanical response of the neat PlasClear-TPGDA, two sets of dogbone samples (gauge section measuring 33 x 5 x 2 mm) were printed, one with their flat side built on the print platform, while the other set had its edge printed on the platform. Both sets had the same layer thickness of 0.05 mm and all other printing parameters were also kept constant. These specimens were loaded in tension to failure using a Zwick-Roell UTM with a 2.5 kN load cell and a cross-head speed of 2.5 mm/min.

Typical stress vs. strain responses obtained for both orientations are plotted in Fig. S5, showing very similar trends. The ultimate strength and fracture strain for both orientations were also observed to be similar, suggesting that the build orientations has no significant influence on the mechanical properties of the printed specimens.

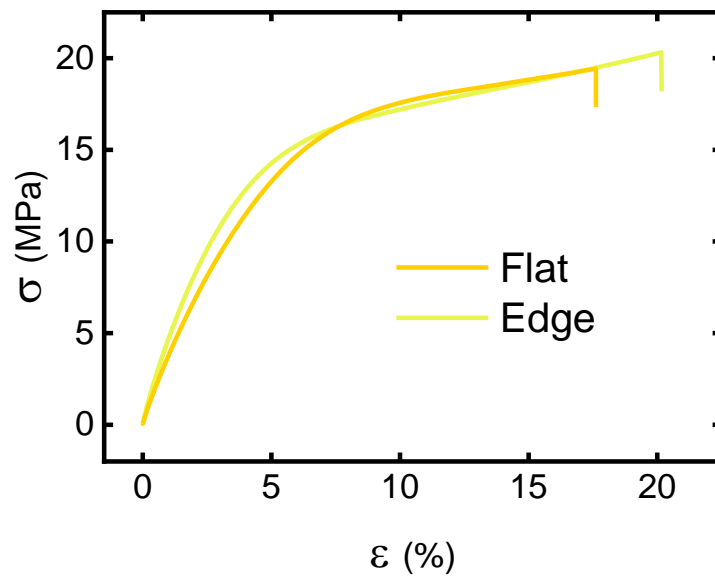


Figure S5. Effect of print orientation on the stress-strain behavior of neat PlasClear-TPGDA.

S4. Effect of post-treatments on the mechanical response

Three types of post-treatments were explored for the 3D printed neat PlasClear-TPGDA: (i) post-curing by exposing the specimen to UV light for 12 min in a UV light chamber, (ii) annealing in an oven at 60°C for 120 minutes followed by cooling in air to room temperature, and (iii) UV curing followed by annealing, as described above. These post-treatments were applied on 3D printed dogbone specimens (gauge section measuring 33 x 5 x 2 mm), keeping all printing parameters fixed. Note that all specimens were rinsed thoroughly with isopropyl alcohol to remove any uncured resin, prior to UV post-curing and/or annealing. The post-treated specimens were subject to uniaxial tensile loading using a Zwick-Roell UTM with a 2.5 kN load cell and a cross-head speed of 2.5 mm/min.

The obtained stress vs. strain curves are plotted in Fig. S6. The UV post-cured specimens showed a much improved Young's modulus and a slightly higher tensile strength than the sample without post-treatments. However, UV post-curing significantly reduced the sample's failure strain, indicating a more brittle response. On the other hand, the annealed specimen showed similar improvements in modulus and strength as the UV post-cured specimen, but had a much higher failure strain, comparable to that of the as-printed specimen. A combination of post-curing and annealing resulted in the highest ultimate strength while achieving a failure strain that lied between those the post-cured and annealed specimens, respectively.

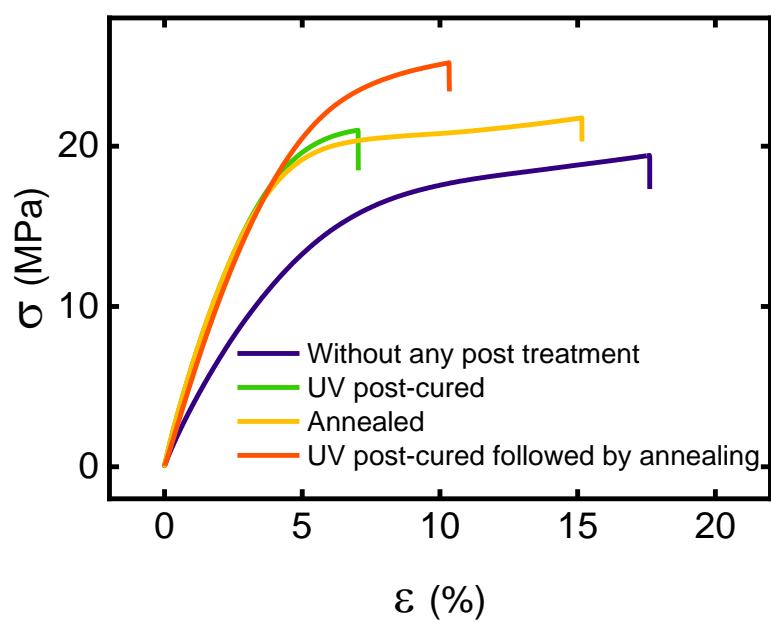


Figure S6. Effect of different types of post-treatments on the stress-strain behavior of neat PlasClear-TPGDA.

S5. Mechanical and piezoresistive response under cyclic tensile loading

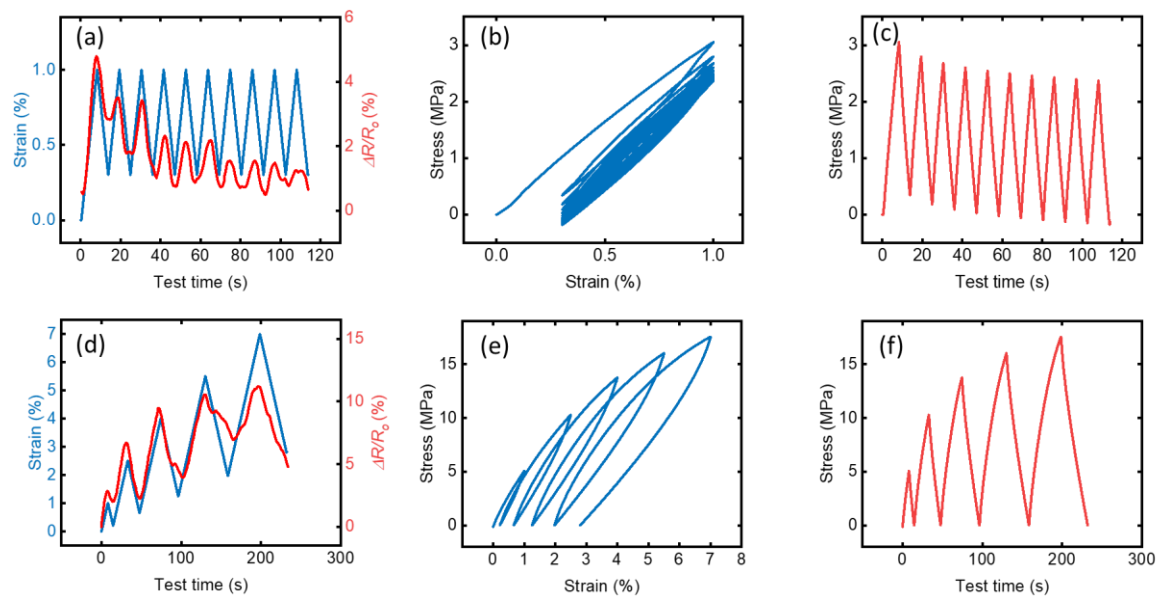


Figure S7. Measurements obtained from cyclic tests with constant (a,b,c) and incrementally increasing (d,e,f) strain amplitudes for PC-0.025.

References

- [1] J. Gotro and R. B. Prime, "Thermosets," *Encycl. Polym. Sci. Technol.*, pp. 1–75, Feb. 2017, doi: 10.1002/0471440264.PST519.PUB2.